2007 IEEE International Conference on
Robotics and Automation
Roma, Italy, 10-14 April 2007

A thermal slip sensor for biorobotic applications

Dino Accoto[†], Francesco Damiani[†], Ranjana Sahai[†],
Domenico Campolo[‡], Eugenio Guglielmelli[‡] and Paolo Dario[†]
[†]CRIM Lab
Scuola Superiore Sant'Anna
Piazza Martiri della Libertà, 33
56127 Pisa, Italy
dino.accoto@sssup.it

[‡]Biomedical Robotics & EMC Lab
Università Campus Bio-Medico
Via Longoni, 83
00155 Roma, Italy
e.guglielmelli@unicampus.it

***Abstract*— This paper presents the design of a novel sensor for slip detection. It consists of an easily fabricated miniaturized thermal probe that senses the additional convective heat transfer associated with the occurrence of mechanical slip. The fabrication procedures and the operating principle for the device are described in detail. A simple experimental setup was used to test the effectiveness of the proposed device. Tests were performed with varying velocities on four materials of differing thermal properties and surface roughnesses. The results show that slip can be effectively detected by the proposed sensor with a response times which can be as low as 6.3 ms. The performance of the device can be further improved when used in conjunction with a separate pressure sensor and by using more accurate methods of electrical resistance measurement.**

I. INTRODUCTION

Fast and accurate detection of slip is crucial in robotic grasping applications, both for artificial manipulators and prosthetic devices. It allows for minimal grasping force, which leads to gentler object handling and power conservation. For effective control purposes, early research in this area [1], [2] recognized the need to detect slip even before the gross event occurred (during what was termed *incipient slip*). Although exact detection time limits are not well quantified in robotic literature, it seems that the best sensors are those that can at least duplicate measured response times in humans ($\approx 65 - 85$ ms [3]).

Many types of phenomena that accompany slip have been exploited for its early detection. Cutkosky et al. [1] noted that incipient slip could be recognized through the vibration of rubber nibs placed on the skin of a grasping device. As the object slipped, periphery nibs would be freed and vibrate. This vibration was detected through embedded accelerometers. Other researchers have made use of detecting vibrations created during slip including using a microphone to record the resulting acoustic signal [4] or sensing it through a thick film PZT cantilever [5] or PVDF film transducers, which were introduced in [6] and applied by embedding them in rubber ridges in [7] and [8]. Dubey and Crowder [9] employed a different phenomenon, a photoelastic effect, to measure slip.

Another slip detection method involved using either one or a combination of measurements from force/torque and tactile sensors. Early work in this area can be found in [10]. Further developments are discussed in [11] and [12]. A variation of this technique involved adding vision feedback to the force and/or tactile data as demonstrated in [13], [14], and [15]. Engel et al. [16] also describes a multi-sensor approach for the development of artificial skin. Here, polymers and thin film metal sensors are utilized to detect surface contour, temperature, thermal conductivity, and hardness, but no systematic method of detecting slip is discussed.

The sensor presented in this paper exploits a thermal phenomenon. By using a thermal probe to detect the additional convective heat transfer associated with the occurrence of mechanical slip (explained further in Sections II and III), it achieves response times as low as 6.3 ms. Compared to the sensors already proposed, this device has some advantages. First, it is able to detect slip independently from surface properties (e.g., roughness) of the touched object, which could even be ideally smooth. Also, as shown in Section IV, thermal properties do not affect the response of the proposed sensor significantly. Additionally, the sensor can be safely mounted on fast moving objects, such as robotic fingers, since mechanical vibrations do not affect it. Finally, since it can be easily manufactured using standard microfabrication processes, it can be further miniaturized to improve its frequency response.

II. DESIGN AND FABRICATION

Slip occurs whenever there is a nonzero relative motion between two objects, say B_1 and B_2, that are in contact. We may imagine that a reference frame is fixed to B_1 (e.g., B_1 may represent a robotic finger) so that the slip velocity is the velocity of B_2 in such a frame. A slip sensor should produce a signal as soon as B_1 observes a nonzero velocity of B_2. The direction and modulus of the actual speed are not required to be measured, nor is other information such as the contact pressure.

The detection strategy we devised employs a thermal probe to be mounted on B_1 and in contact with B_2. The probe is heated by joule effect and kept at a constant temperature that exceeds normal room temperature. The heat generated in the probe is dispersed in the surrounding environment, and the electrical power supplied to the probe equals the rate of heat dispersion.

The thermal problem can be formulated using the well known Fourier equation:

$$\frac{\partial T}{\partial t} = \kappa \nabla^2 T + q(\mathbf{x}) \tag{1}$$

where $q(\mathbf{x})$ is the thermal source and $\kappa = \frac{k}{c_p \rho}$ is the thermal diffusivity (m^2/s) in which k, c_p and ρ respectively are the thermal conductivity (W/mK), the specific heat (J/kgK), and the density (kg/m^3).

When B_2 slips, a convection term must be added to (1), so we have:

$$\frac{\partial T}{\partial t} + \mathbf{v} \cdot grad\, T = \kappa \nabla^2 T + q(\mathbf{x}) \tag{2}$$

where $\mathbf{v}$ is the slip velocity.

Given that the temperature of the sensor is constant, the addition of convection ($\mathbf{v} \cdot grad\ T$ term in (2)) causes an increase in the heat generation (proportional to the $q(\mathbf{x})$ term), which can be controlled electrically. The working principle is illustrated in Fig. 1.

Keeping the thermal probe at constant temperature is greatly beneficial for its sensitivity. Once the sensor itself and its support (e.g., a robotic finger) reach a thermal steady state, quick power absorption changes can be recognized to be caused only by comparably quick phenomena, such as tactile events. On the contrary, slow phenomena can be easily discarded as spurious events (e.g., environment temperature changes). Exactly how the power changes are translated into slip detection by the sensor is described in detail in Section III-A.

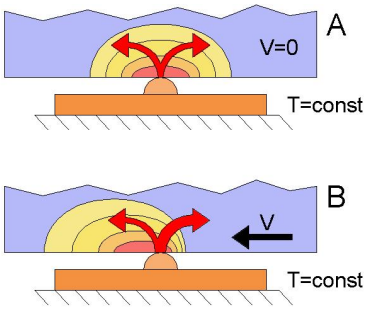

Fig. 1. The motion of the object (B) enhances the heat transfer by introducing a convective transport, while only conduction occurs if the object is at rest (A).

Miniaturization is a key issue in order to have a fast-responding sensor. Indeed, thermal phenomena, if compared to electromechanical phenomena, are, in general, relatively slow. Given a body of length L and cross section S, its thermal time constant is of the order of $1/RC$ where $R = \frac{1}{k} L/S$ is the thermal resistance and $C = LS\rho c_p$ is the thermal capacity. For a given material the time constant is therefore proportional to L^{-2}, which means that response time becomes smaller as the linear dimension of the body diminishes. This explains why we used lithographic techniques to microfabricate the sensor.

The electrical parts of the sensor have been fabricated over a square glass substrate (25×25 mm^2), 960 μm thick. They comprise a resistor and four electrical connections (Fig. 2). The electrical parts were patterned by a standard lift-off process using Shipley S1813 photoresist. The resistor was fabricated by patterning a 16 nm Au layer over a 5 nm Cr adhesion layer. The resistor is inscribed in a 1 mm diameter circle and the width of the wire is 70 μm. The electrical contacts were constructed by sandwiching a 10 nm Ti adhesion layer, a 100 nm Au conduction layer and 20 nm Ti oxide protection layer. The whole surface of the sensor was then spin-coated with a 10 μm layer of polyimide, which was photopatterned to keep the pads accessible (see Fig. 3). To localize the thermal contact, a small cyanoacrylic drop was deposited over the micro-heater. The drop is about 40 μm high and approximately 1 mm wide (Fig. 3).

Gold was chosen for the micro-heater since it has a positive electrical resistivity coefficient, meaning that its electrical resistivity increases with temperature. This feature has been used to detect temperature via electrical measurements, with no need for dedicated temperature sensors, such as thermocouples.

By using a K thermocouple and a Delta OHM meter (Model HD9016) we measured how the resistance changes with temperature. The data can be fit using a linear regression with very high confidence ($\sigma^2 = 0.992$):

$$R = 0.735T + 366.46 \tag{3}$$

where temperature (T) is in degrees centigrade and resistance (R) is in Ω.

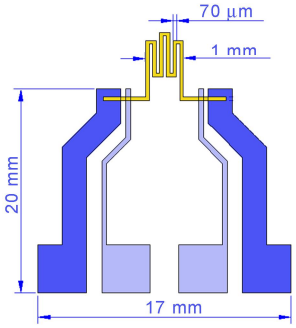

Fig. 2. Geometry of the sensor's electrical parts (not to scale).

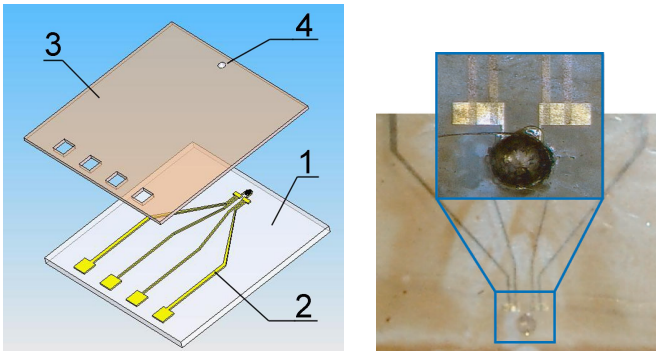

Fig. 3. *(left)* Exploded view of the sensor assembly. 1: glass support; 2: electrical parts; 3: polyimide protection layer; 4: cyanoacrylate drop. *(right)* Close-up of fabricated sensor.

III. EXPERIMENTAL SETUP AND PROCEDURE

A. Control

A dedicated control system takes care of keeping the micro-heater temperature at a constant value ($49.5\,^{\circ}\mathrm{C}$). This temperature was chosen because it is above that of most objects we commonly handle, while still being low enough not to cause unbearable discomfort in case of prolonged contact with the human skin.

The sensor has four connections: two for applying a current (the wider connections shown in Fig. 2) and the other two (the thinner connections shown in the same figure) to sense the voltage drop across the micro-heater.

Given that the current supplied is known, it is straightforward to calculate the resistance as $R = V/I$, where V is the voltage drop measured. Then the electrical resistance can be converted into a temperature according to the experimentally determined equation given in Eq. (3).

The control system connected to the sensor (depicted in Fig. 4) is comprised of a National Instruments DAQ card E6062 connected to a PC and to two external circuits. The first circuit is for generating a constant current proportional to an input voltage provided by the DAQ analog output (AO). The other circuit is a differential amplifier that adapts the voltage coming from the device to the voltage limits of the DAQ analog input (AI) (+10V,-10V) and separates the device from the ground of the DAQ. Both the circuits are powered by an Agilent E3634A power supply.

The current supplied to the micro-heater can have two intensities: a lower one (I_L) and a higher one (I_H). Every T_s seconds the resistance of the micro-heater is read and compared to the reference resistance (403Ω) corresponding to the target temperature ($49.5\,^{\circ}\mathrm{C}$). If the resistance (temperature) is found to be below the reference value, current is switched to I_H, otherwise to I_L. Then, the current is kept constant until the next resistance measurement and comparison are made (Fig. 5).

The period T_s can be chosen quite freely, provided it is short compared to the thermal time constant. We experimentally found that $1 < T_s < 8$ ms is an acceptable range. The time required to measure the resistance is on the order of a few microseconds, and it is much shorter than T_s. This allowed us to collect two resistance measurements before every cycle and to calculate their mean value, thus, greatly improving the readout of the sensor. Table I summarizes the electrical parameters used in the experiments.

$T_s\,(ms)$	$I_H\,(mA)$	$I_L\,(mA)$
6	17	5
2	17	7

TABLE I

ELECTRICAL OPERATIONAL PARAMETERS USED IN THE EXPERIMENTS.

B. Slip Detection Algorithm

For each slip test, the values of the current fed to the sensor were recorded in a file for off-line analysis, using a

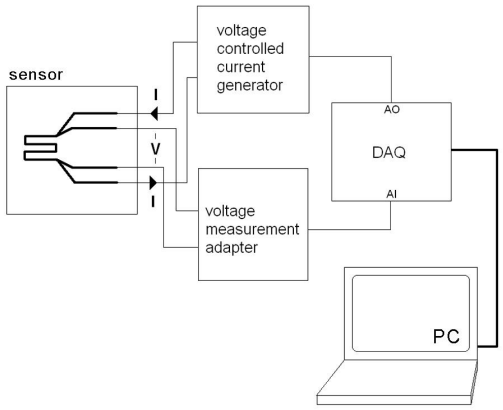

Fig. 4. Control and measurement set-up.

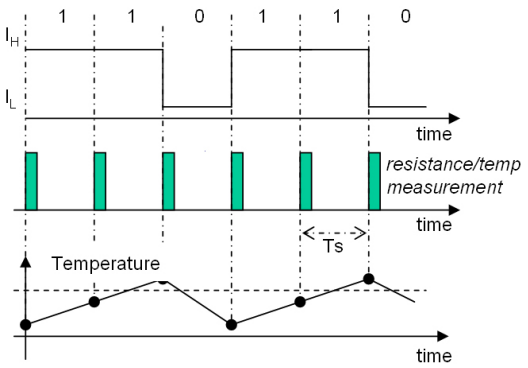

Fig. 5. Depiction of control scheme based on measured resistance / temperature.

binary codification in which 1 stands for I_H and 0 for I_L. To detect the onset of slip, we should look for a procedure to effectively evaluate the power increase associated with slip using a computationally less intensive method.

As shown in Fig. 1, when slip occurs, more power is required to keep the heater at a constant temperature. We therefore wish to count the time the heater *continuously* stays "ON".

To this end, since the I_n denotes the powering sequence (the heater is "ON" if $I_n = I_H$ or "OFF" if $I_n = I_L$) during each time interval $(n-1)T_s < t < nT_s$, we defined a counting variable N as follows:

- $N = 0$ if $I_n = I_L$;
- $N = N + 1$ if $I_n = I_H$;

starting from $N = 0$ as initial condition.

This allows estimating the time $N\,T_s$, i.e. the time during which the heater is continuously "ON".

A time threshold T_0 should be determined so that if $N\,T_s \geq T_0$, the sensor fires a signal. N is a stochastic variable and, although unlikely, it is possible to have $N\,T_s \geq T_0$ even without any slip (false positives). As with any stochastic variable, N can be empirically characterized in terms of a mean value $\bar{N}$ and variance σ_N. The threshold T_0 should be set as $T_0 = T_s(\bar{N} + x\sigma_N)$ where the larger x means a smaller chance of having false positives but, at

the same time, a higher bound on the lowest detectable slip speed.

C. Experimental set-up

To test the effectiveness of the proposed method of slip detection, a series of experiments were performed. Fig. 6 depicts the basic experimental setup. The slip sensor was placed on a z-stage with two block supports on either side. A bar of rectangular cross-section and a given material was placed across the slip sensor such that the blocks on the sides supported either end of the bar. This bar was then slid horizontally to produce the slip to be detected by the sensor. The surfaces of the supports were chosen to be smooth so that the friction between the sliding bar and the surfaces was minimal.

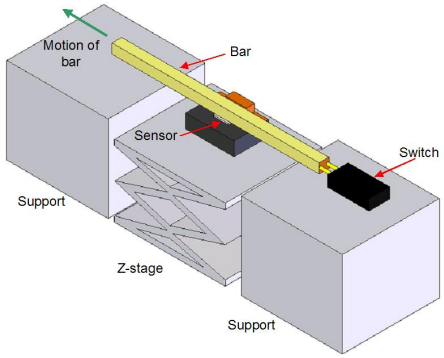

Fig. 6. Experimental setup for measuring slip.

A switch mechanism was implemented at one end of the bar. This switch consisted of two sharp metal contacts. One contact was rigid, and other was longer but spring-loaded. The end of the bar, which was covered with a layer of copper shim, was pushed against the spring-loaded contact until it touched the rigid contact. With this setup, the opening of the switch recorded the instant the bar began to slip. Data from both the switch and slip sensor were captured using LABVIEW and the already cited data acquisition card.

The sensor was operated as described in Section III-A. A bar of a given material was put into position on the block supports and against the switch. The z-stage under the sensor was then raised to make contact with the bar. After achieving equilibrium with the sensor, the bar was slid to detect slip. The bar was put into motion using a motor pushing a ratchet that then propelled the bar. Different size gears were used to produce varying velocities. Other velocities were also achieved by sliding the bar by hand steadily a set distance in a given amount of time. Tests of slip with various velocities were performed for four different kinds of materials: Teflon (polytetrafluoroethylene), pine wood, Delrin (polyoxymethylene), and polystyrene.

The thermal properties of the selected materials, summarized in Table II, were taken from the manufacturers' datasheets, with the exception of those for the pine wood. For these, the density of the wooden bar was measured, while its thermal properties were taken from [17] assuming an ambient humidity of 40%.

Material	Thermal conductivity, $k\ (W/mK)$	Specific heat, c_p (J/kgK)	Density, ρ (kg/m^3)	Thermal diffusivity, κ $(\times 10^{-7} m^2/s)$
Teflon	0.245	1172	2180	0.96
Wood	0.12	1674	542	1.32
Delrin	0.31	1465	1370	1.54
Polystyrene	0.17	1300	1050	1.25

TABLE II

THERMAL PROPERTIES OF THE MATERIALS USED FOR SLIP TESTS.

The results of these tests are discussed in the following section.

IV. RESULTS

Note that, in terms of the I_n vector described earlier, the instantaneous power dissipated by the heater is: $P_n = RI_n^2$ while the energy supplied to the sensor up to cycle n can be computed as: $E_n = E_{n-1} + P_{n-1}T_s$.

Since the sensor is warmer than the surrounding environment, E_n grows steadily with n. On the contrary, P_n reaches a plateau after a transient and remains constant until slip occurs. Along the plateau power is dissipated through the sensor mounting and the bar, which is in contact with the sensor. This power depends, in general, on the thermal conductivity of the touched object, as shown in Fig. 7. From the plot we notice that a constant power (57.39 mW), expectedly dissipated through the mounting, does not depend on the type of material, while the other ($34.52\,k$) is dissipated through the touched objects and depends upon their thermal conductivity.

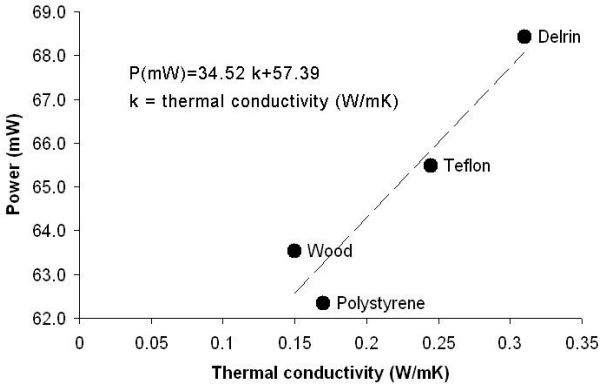

Fig. 7. Power dissipated by the sensor at steady-state conditions.

Subtracting such power from that provided to the sensor highlights the energy absorbed during slip (Fig. 8) and the increase in absorbed power during slip (Fig. 9). As expected from Eq. (2) power absorption is an increasing, nonlinear function of slip speed (Fig. 9), but it does not depend significantly on the thermal properties of the materials.

Although we may expect that materials with higher thermal diffusivity would spread heat more efficiently than less conductive materials, we can see from Fig. 8 that the power

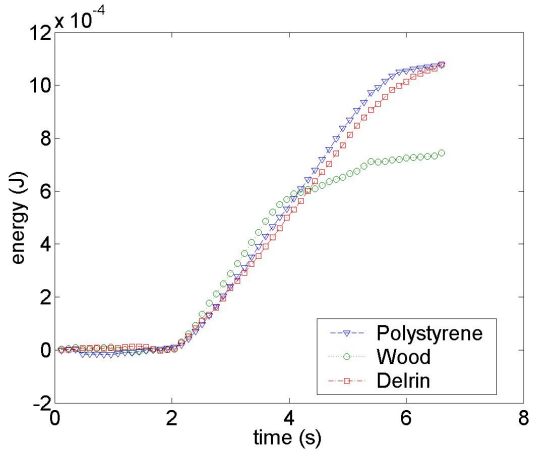

Fig. 8. Energy absorption related to slip for three materials. Common slip velocity: 28.3 mm/s.

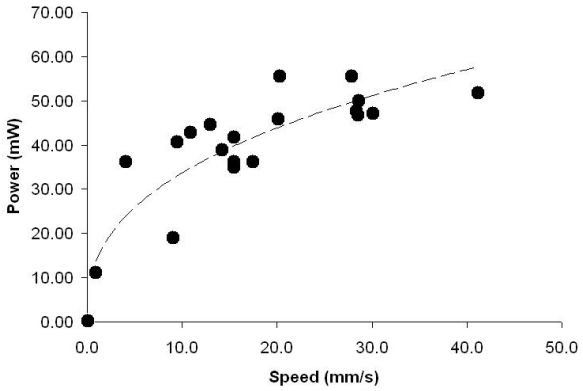

Fig. 9. Power absorbed as a consequence of the start of slip. Different materials do not behave in a significantly different way.

absorbed during slip, i.e. the slopes of the three linear tracts, is not ordered accordingly. This may be due to the different surface roughness of the four bars used during the tests, which could affect the quality of the thermal contact since smoother surfaces should allow for better contact.

Fig. 10 presents a typical plot of sensor data obtained for the same material (polystyrene) at three different slip speeds. We should note that the full shape of the plot is for illustration purposes only, since the sensor indicates slip as soon as the measured delay increases. As expected, we can see that longer delay times, i.e. higher power absorption, correspond to higher slip speeds.

The response time of the sensor is the time required for the thermal perturbations due to slip to propagate and reach a minimum detectable level. The response time depends greatly on the working conditions, which have been already reported in Table I. In particular, the response time appears to be very sensitive to the sampling time T_s. For example, the average response time for the operational parameters given in the first row of the table was 154 ms, while when changed to the parameters in the second row, the response time was 6.3 ms. Considering that an average speed of 15 mm/s was used during the tests, the slip distance between detection for the two cases were respectively 2.3 mm and 0.1 mm.

Fig. 11 shows a close up of a delay plot. The red line indicates the time at which the switch was opened (the inception of slip) and the green line indicates the time at which the sensor detects the slip. The time difference between lines, or the sensor's response time, in this case was approximately 40 ms, comparable with that of human sensors [3].

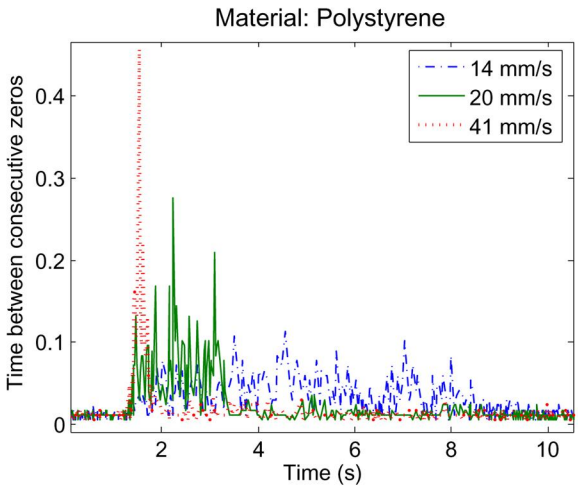

Fig. 10. Delay plots for polystyrene. Slip occurs at three different speeds.

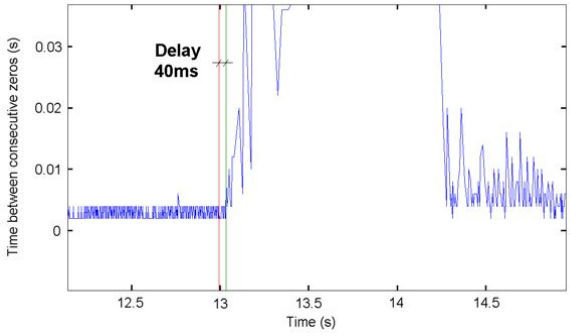

Fig. 11. Detail of a delay plot showing slip.

V. CONCLUSIONS AND FUTURE WORK

A. Conclusions

In this paper we presented a slip sensor based on a novel working principle. The sensor is kept at a constant temperature slightly above the room temperature ($\approx 50\,^{\circ}\mathrm{C}$). When slip occurs, the sensor balances the increase in heat removal due to convective heat transport with an increased generation of thermal power by the micro-heater. When such increase overcomes a given threshold, a slipping signal is fired.

As can be evaluated from the interpolated data reported in Fig. 7, the maximum power dissipated through the touched object is of the order of 10 mW. Such a small value

guarantees that most objects can be touched safely since the thermal effects on them are very limited[1].

The sensor has been tested with four materials of different thermal properties. Experimental results showed that it is able to detect slip with an average response time as low as 6.3 ms, which corresponds to slip lengths of the order of 0.1 mm. Further miniaturization should allow for even better performances.

The sensor is compact (the gold micro-heater is also used as temperature sensor) and with no moving parts. It is insensitive to spurious mechanical vibrations, and it can be mounted on moving robotic fingers.

B. Future Work

One of the main issues of the sensor is that it is not able to discriminate between a slipping event and a contact event. When an object is initially put in contact with the sensor, the sensor will show a thermal variation. When the contact pressure between the object and sensor changes, a thermal variation will also occur, because the area of the contact surface between the sensor and the object increases with pressure, thus favoring heat exchanges.

To avoid the ambiguities which could arise from this, a pressure sensor that has a different working principle can be used in conjunction with the thermal sensor. By mounting the two sensors in close proximity to each other, they can be used to decide if slip is occurring or if it is a contact or pressure variation. The pressure sensor should detect contact and pressure variation events so that the thermal sensor signals can be discarded at those times. When the pressure sensor is not detecting an event and the thermal sensor detects a variation, it means that a slipping event is occurring. The use of a pressure sensor can also give information for the case of two contemporaneous events of different types. For example, if the sensors are in put in contact with an object and both detect an event, the slipping should be discarded. However, if, in the meanwhile, the object is also slipping, then the thermal transient is not the same as the case of contact alone. By comparing the thermal transient with the expected transient for simple contact, the slipping event can be detected. The same reasoning can be applied if there is a pressure variation and slip occurring simultaneously.

A lesser issue involves the response time of the sensor. Although the sensor response time can be as small as 6.3 ms, better performance can be achieved by improving the resistance readings. Indeed, the error on resistance (i.e. 2σ), evaluated on the experimental data, is 0.2Ω. Since resistance is directly proportional to temperature, the noise on the temperature is $0.3\,^{\circ}\mathrm{C}$. Temperature changes lower than this value cannot be distinguished. By improving the quality of resistance measurements, lower temperature changes could be detected by the control system, with benefits on the response time.

[1]Such a low power would require more than 6 min to increase the temperature of 1 gram of water by $1\,^{\circ}\mathrm{C}$.

VI. ACKNOWLEDGMENTS

We would like to thank Mr Francesco Leone for having co-operated on the development of a preliminary version of the device, intended to prove the feasibility of a pressure/contact sensor based on thermal phenomena (unpublished).

REFERENCES

[1] M. R. Cutkosky and J. M. Hyde, "Manipulation control with dynamic tactile sensing," *International Symposium of Robotics Research*, October 1993.

[2] M. C. Tremblay and M. R. Cutkosky, "Estimating friction using incipient slip sensing during a manipulation task," *IEEE International Conference on Robotics and Automation*, pp. 429–434, May 1993.

[3] G. Westling and R. S. Johansson, "Responses in glabrous skin mechanoreceptors during precision grip in humans," *Experimental Brain Research*, vol. 66, pp. 128–140, 1987.

[4] P. J. Kyberd, M. Evans, and S. Winkel, "An intelligent anthropomorphic hand with automatic grasp," *Robotica*, vol. 16, pp. 531–536, 1998.

[5] A. Cranny, D. P. J. Cotton, P. H. Chappell, S. P. Beeby, and N. M. White, "Thick-film force and slip sensors for a prosthetic hand," *Sensors and Actuators A*, vol. 123-124, pp. 162–171, 2005.

[6] P. Dario, C. Domenici, R. Bardelli, D. DeRossi, and P. C. Pinotti, "Piezoelectric polymers: new sensor materials for robotic applications," *13th International Symposium on Industrial Robots and Robots*, vol. 2, pp. 14.34–14.49, 1983.

[7] I. Fujimoto, Y. Yamada, T. Morizono, Y. Umetani, and T. Maeno, "Development of artificial finger skin to detect incipient slip for realization of static friction sensation," *Multisensor fusion and integration for intelligent systems*, pp. 15–20, 2003.

[8] B. Choi, H. R. Choi, and S. Kang, "Development of tactile sensor for detecting contact force and slip," *IEEE/RSJ International Conference on Intelligent Robots and Systems*, pp. 2638–2643, 2005.

[9] V. N. Dubey and R. M. Crowder, "A dynamic tactile sensor on photoelastic effect," *Sensors and Actuators A*, vol. 128, pp. 217–224, 2006.

[10] A. Bicchi, J. K. Salisbury, and P. Dario, "Augmentation of grasp robustness using intrinsic tactile sensing," *IEEE International Conference on Robotics and Automation*, pp. 302–307, 1989.

[11] C. Melchiorri, "Slip detection and control using tactile and force sensors," *IEEE/ASME Transactions on Mechatronics*, vol. 5, pp. 235–243, 2000.

[12] N. Tsujiuchi, T. Koizumi, A. Ito, H. Oshima, Y. Nojiri, Y. Tsuchiya, and S. Kurogi, "Slip detection with distributed-type tactile sensor," *IEEE/RSJ International Conference on Intelligent Robots and Systems*, pp. 331–336, 2004.

[13] T. Hasegawa and K. Honda, "Detection and measurement of fingertip slip in multi-fingered precision manipulation with rolling contact," *Sensor Fusion for Intelligent Systems*, 2001.

[14] K. Hosoda, Y. Tada, and M. Asada, "Internal representation of slip for a soft finger with vision and tactile sensing," *IEEE/RSJ International Conference on Intelligent Robots and Systems*, pp. 111–115, October 2002.

[15] A. Ikeda, Y. Kurita, J. Ueda, Y. Matsumoto, and T. Ogasawara, "Grip force control for an elastic finger using vision-based incipient slip feedback," *IEEE/RSJ International Conference on Intelligent Robots and Systems*, pp. 810–815, 2004.

[16] J. Engel, J. Chen, Z. Fan, and C. Liu, "Polymer micromachined multimodal tactile sensors," *Sensors and Actuators A*, vol. 117, pp. 50–61, 2005.

[17] "Thermal conductive properties of wood, green or dry, from -40 deg to +100 deg c: a literature review," USDA Forest Service General Technical Report, 1977.